A summary of the paper: "Water storage changes and climate variability within the Nile Basin between 2002-2011", Advances in Water Resources, doi:10.1016/j.advwatres.2014.06.010

J.L. Awange[a,c], E. Forootan[b,1], M. Kuhn[a], J. Kusche[b], B. Heck[c]

[a] *Western Australian Centre for Geodesy and The Institute for Geoscience Research Curtin University, Perth, Australia*
[b] *Institute of Geodesy and Geoinformation, Bonn University, Bonn, Germany*
[c] *Geodetic Institute, Karlsruhe Institute of Technology, Karlsruhe, Germany*

Abstract

The Gravity Recovery And Climate Experiment (GRACE) satellite mission provides a unique opportunity to monitor changes in total water storage (TWS) of large river basins such as the Nile. Use of GRACE-TWS changes for monitoring the Nile is, however, difficult since stronger TWS signals over the Lake Victoria Basin (LVB) and the Red Sea obscure those from smaller sub-basins making their analysis difficult to undertake. To mitigate this problem, this study employed Independent Component Analysis (ICA) to extract statistically independent TWS patterns over the sub-basins from GRACE products. Such extraction enables an in-depth analysis of water storage changes within each sub-basin and provides a tool for assessing the influence of anthropogenic as well as climate variability caused by large scale ocean-atmosphere interactions such as the El Niño Southern Oscillation (ENSO) and the Indian Ocean Dipole (IOD). Our results indicate that LVB experienced effects of both anthropogenic and climate variability during 2002-2011 coinciding with the drought that affected the Greater Horn of Africa. Ethiopian Highlands (EH) generally exhibited a declining trend in the annual rainfall over the study period. A correlation of 0.56 was found between ENSO and TWS changes over EH indicating ENSO's dominant influence. TWS changes over Bar-el-Ghazal experienced mixed increase-decrease, with ENSO being the dominant climate variability in the region during the study period. A remarkable signal is noticed over the Lake Nasser region indicating the possibility of the region losing water not only through evaporation, but also possibly through over extraction from wells in the

Email addresses: `J.Awange@curtin.edu.au` (J.L. Awange), `forootan@geod.uni-bonn.de` (E. Forootan)

[1] Address for corresponding author (Ehsan Forootan): Institute of Geodesy and Geoinformation, Bonn University, Nussallee 17, D53115, Bonn, NRW, Germany, Tel: 0049228736423, Fax: 0049228733029, E-mail: forootan@geod.uni-bonn.de

Western Plateau (Nubian aquifer).

Key words: Nile Basin, Lake Victoria, Ethiopian Highlands, Bar-El-Ghazal, GRACE- total water storage, climate variability

---

1. Introduction

To support the management of the Nile Basin's water resources, it is essential to understand the changes in its stored water (surface, groundwater, and soil moisture) and their relation to climate variability such as the El Niño Southern Oscillation (ENSO) and the Indian Ocean Dipole (IOD). Due to its large spatial extent, however, changes in Nile Basin's stored water cannot be monitored using traditional methods (e.g., piezometric-based). This calls for satellite based methods of observation. One such satellite is the Gravity Recovery And Climate Experiment (GRACE) whose use offers a unique chance to monitor changes in the total water storage (TWS, i.e., an integral of surface, groundwater, and soil moisture storage) within the Nile Basin (see, e.g., Awange et al. , 2008, 2013a,b; Becker et al. , 2010; Bonsor et al. , 2010; Senay et al. , 2009; Swenson and Wahr , 2009; Longuevergne et al. , 2012).

The main challenges in using GRACE-TWS changes over the Nile Basin is that on the one hand, the derived hydrological signals are dominated by stronger signals, e.g., those around the lakes such as Lakes Victoria and Tana (see, e.g., Awange et al. , 2013b), as well as regions close to the Red Sea and the Mediterranean Sea (Aus der Beek et al. , 2012). Computing basin average water variations, therefore, is normally influenced by dominant signals such as that of Lake Victoria Basin (LVB), while the relatively weaker signals from the other regions are masked making analysis of changes in TWS over such sub-basins difficult. On the other hand, Rodell and Famiglietti (2001) pointed to the limitation of GRACE products to study basins of less than 200,000 km^2. Since some of the Nile's sub-basins (e.g., Lake Nasser region) have areas less than 200,000 km^2, thus, computing TWS changes of them is limited by the spatial resolution of GRACE (e.g., 400,000 km^2 in Swenson et al. (2003) and Tapley et al. (2004)). Previous analysis of the Nile basin based on the GRACE satellite data have thus been unable to separate the signals into their respective sub-basins for the purpose of providing an in-depth analysis of spatial variations (see, e.g., Awange et al. , 2013b).

To overcome these challenges, in the present study; (i) we apply a higher order statistical tool of Independent Component Analysis (ICA) (Spatial ICA in Forootan and Kusche , 2012, 2013) over the Nile Basin (between 10° S to 35° N and 25° E to 45° E) to separate GRACE-TWS changes between 2002 to 2011 into their spatially independent sources (i.e., sub-basins). This is then followed, in (ii), by an evaluation of the impacts of global climate change on the TWS within these sub-basins using global climate forcing by IOD and ENSO.

2. The Nile Basin

The Nile Basin (Fig. 1) has two major tributaries, the White Nile and the Blue Nile, the latter being the main source of its water. The White Nile originates from the Great Lakes region of Eastern Africa, and flows northwards through Uganda and South Sudan. The Blue Nile on the other hand starts from Lake Tana in the Ethiopian Highlands (EH), flowing into Sudan from the southeast and meets the White Nile at Khartoum in Sudan. From there, the Nile passes through Egypt, which is mostly dry (i.e., 92%) and Sudan, and finally discharges into the Mediterranean Sea (see, e.g., Sahin , 1985).

The four main areas of interest to our study, whose changes in TWS could be remotely sensed using GRACE satellite data due to their larger spatial coverage (i.e., over 200,000 km^2) are (see Fig. 1): (i) Lake Victoria Basin (LVB), which is the headwaters of the White Nile; (ii) the Bahr-el-Ghazal region (BEG), the main western tributary of the Nile, and the largest sub-basin. Its supply to the Sudd wetlands is however reported by Mohamed et al. (2006) to be negligible. Nonetheless, it is included in this study to assess the impacts of climate variability on its TWS changes. The Sudd wetlands (marshes) is the region between Mongalla and Malakal, which consists of marshes and lagoons, and is believed to be where most of the White Nile's water is lost due to evaporation (Yates , 1998); (iii) the Ethiopian Highlands (EH), and the headwaters of the Blue Nile; and (iv) the Egyptian desert region consisting of Lake Nasser, where significant amounts of water are lost due to evaporation (see details of regions in Conway and Hulme , 1993). The characteristics of these regions are summarized in Table (1).

FIGURE 1

3. Data and Methodology

3.1. Data

The data used in this study consisted of remotely sensed GRACE-TWS changes from 2002 to 2011, Tropical Rainfall Measuring Mission (TRMM)-derived precipitation, and water storage data from Global Land Data Assimilation System (GLDAS) hydrological model over the same period.

3.1.1. Gravity Recovery And Climate Experiment (GRACE)

GRACE products of GFZ Potsdam (Flechtner , 2007) are provided at monthly resolutions and consist of a set of fully normalized spherical harmonic coefficients of the geopotential, up to degree and order 120. These coefficients are contaminated by correlated errors, manifesting as stripes in the spatial domain. These striping and high-frequency effects potentially mask hydrological signals, making their detection extremely difficult (e.g., Kusche , 2007; Awange et al. , 2009). In this regard, the GFZ solutions were smoothed using the DDK2 de-correlation filter (Kusche et al. , 2009)[2].

---

[2](http://icgem.gfz-potsdam.de/ICGEM/TimeSeries.html)

In order to derive the TWS changes, residual gravity field solutions taken with respect to 9 years average were derived. The resulting residual geopotential coefficients were then transformed into monthly TWS changes using Wahr et al. (1998)'s approach. Besides the total signals of the respective sub-basins, this study explored the possibility of analyzing the residual signals once the dominant signals of Lake Victoria, Lake Tana and the Red Sea were removed. To remove the lakes' signals from GRACE-TWS changes, we followed the approach in Swenson and Wahr (2002). The surface height of each lake was assumed to be changing homogeneously. For each lake, a global grid was defined by a function f, where its surface was given a value 1 and 0 over the rest of the globe (i.e., equivalent to 1 mm Equivalent Water Thickness (EWT) over the lake and zero over the rest of the globe). The altimetry data were downloaded from the LEGOS website (http://www.legos.obs-mip.fr/en/soa/hydrologie/hydroweb/). As an example, in Fig. 2, the satellite altimetry-derived EWT changes and GRACE-TWS time series corresponding to Lake Victoria over the period 2002 to 2011 are shown.

FIGURE 2

3.1.2. El Niño and Southern Oscillation (ENSO)

See the description of the ENSO impact on TWS changes in the final paper. This study used monthly Southern Oscillation Index (SOI) provided by the Australian Bureau of Meteorology covering the period from 2002 to 2011[3].

3.1.3. Indian Ocean Dipole (IOD)

See the description of the IOD impact on TWS changes in the final paper. In this study, we used DMI time series provided by the Japan Agency for Marine-Earth Science and Technology (JAMSTEC) covering the period from 2002 to September 2010[4].

3.2. Methodology
3.2.1. Extracting Independent Patterns

In order to assess the water storage changes within the Nile Basin, the Spatial Independent Component Analysis (Spatial ICA) approach (see, Forootan and Kusche , 2012; Forootan et al. , 2012) was used to extract the spatially independent signals within the Nile Basin boundary, selected to extend from $25°$E $< \lambda < 45°$E and $5°$S $< \varphi < 35°$N, including areas that do not actually belong to the Basin, such as the Red Sea (Fig. 1). For instance, assuming that time series of TWS fields, after removing their temporal mean, are stored in a matrix $\mathbf{X}_{TWS} = \mathbf{X}_{TWS}(t, s)$, where t is the time, and s stands for spatial

---

[3](http://www.bom.gov.au/climate/enso/)
[4](http://www.jamstec.go.jp)

4

coordinate (grid points). Applying Spatial ICA, $\mathbf{X}_{TWS}$ can be decomposed into spatial and temporal components as

$$\mathbf{X}_{TWS} = \mathbf{A}_j \mathbf{S}_j, \tag{1}$$

where $\mathbf{A}_j$ $(t \times j)$ stores the j dominant unit-less temporally evolution of TWS changes in its columns, and the rows of $\mathbf{S}_j$ $(j \times s)$ represent their corresponding statistically independent spatial maps. Each temporal pattern (a column of $\mathbf{A}_j$) along with its corresponding spatial pattern (a row of $\mathbf{S}_j$) provides an independent mode of variability (Forootan and Kusche , 2012, 2013). The use of the Spatial ICA method, which is simply called ICA from now on, is advantageous in two respects: first, it localizes the signals and isolates those outside the basin; and second, it provides statistically independent components, which enhance the interpretation of the results.

To understand the advantages of using ICA in localizing TWS changes over the Nile Basin, let us use a simple illustration of Fig. 3 based on simulated data. Let us assume that the water storage changes of the Nile Basin consists of changes in lake water storage, soil moisture, and sea storage. We demonstrate the power of the ICA (Forootan and Kusche , 2012) in a two-step approach (see, also Forootan et al. (2012) for a simulation example on Australia). In the first step, we simulate the combined lake water storage, soil moisture, and sea storage over the Nile Basin and in the second step, we apply the ICA approach to localize them into their respective separate components. To achieve the first step, altimetry data from the LEGOS website (Crétaux et al. , 2011) are used to introduce the Lake water storage changes, which are then converted to EWT using the approach discussed in section 3.1.1. The same approach is used to covert the level variations of the Red Sea[5] into EWT changes, while the soil moisture are introduced from the GLDAS model (see the full paper). From the first step, Fig. 3(top-A) shows the introduced signals of lakes, Fig. 3(top-B) corresponds to soil moisture changes, and Fig. 3(top-C) represents the introduced signals over the sea. Combined, Figs. 3(top-A,B, and C) leads to Fig. 3(top-D) that contains a summation of all the signals. As can be seen from Fig. 3(top-D), the composition of the mixed signals make it hard to interpret thereby necessitating the need for ICA method to separate them and make them interpretable.

The combined patterns of Fig. (3, top-D) are decomposed by ICA method in order to identify the sources, the results of Fig. (3, bottom) show that the introduced water storage changes over the Red Sea and Lake Nasser having been separated as the first independent mode (IC1). Soil moisture pattern are extracted as the second independent mode (IC2), and finally, water storage changes of Lake Vitoria are localized in the third independent mode (IC3). The successful performance of ICA in localizing the simulated water storage changes motivated its application to real GRACE-TWS data over the Nile Basin. For

---

[5](from http://coastwatch.pfeg.noaa.gov)

more discussion on the ICA-method, its performance on decomposing GRACE-derived TWS fields, as well as its comparison with the second order statistical method of Principal Component Analysis (PCA), we refer to Forootan and Kusche (2012) and Forootan et al. (2012, 2014). In the paper, the main independent patterns of GRACE/GLDAS-derived TWS changes are compared to those of TRMM rainfall (considered as the main input of TWS changes over the Nile Basin).

FIGURE 3

4. Results

4.1. Comparisons of GRACE-TWS, GLDAS-TWS, and TRMM-Rainfall Changes

Implementing ICA on GRACE-TWS changes produced 4 significant spatially independent components over the study region corresponding to 92% of the cumulative total variance of TWS changes (see Fig 4). Figure 4 shows the first independent mode (spatial and temporal patterns of IC1) of GRACE to be localized over the BEG region (dominated by an annual signals), the second independent mode (IC2) is localized over the EH, the third independent mode (IC3) over LVB, and finally the fourth independent mode (IC4) is found to be over the Red Sea and the northern parts of the basin. In comparison, we sho results of ICA when it is applied to GLDAS and TRMM sata sets in the paper. The first mode of GLDAS captures a similar pattern over the BEG, and the anomalies over the northeast part of the LVB. It, however, shows a weaker signal over EH. Applying ICA to rainfall variability of basin, indentifies the rainfall signal over LVB in the first mode (IC1) and EH in the second mode (IC2). It does not show any rainfall related fluctuations over the Red Sea.

With the removal of Lake Victoria's signal using the procedure discussed in section (3.2), the TWS from GRACE data did not change for BEG but is concentrated more over the catchments for LVB and EH (Fig. 5). For the Nasser region, the removal of the Red Sea and the Lake Nasser signal allowed the possible impact of ground water extraction in the the Western Plateau (Nubian aquifer; e.g., Sultan et al. , 2012) to be more visible (e.g., Fig. 6). The results of correlations between TWS changes in different sub-basins and the climate variability of ENSO and IOD are summarized in Table 2.

FIGURE 4

FIGURE 5

4.2. Analysis of stored water and climate variability over the sub-basins

4.2.1. Bahr-el-Ghazal region (BEG)

Bahr-el-Ghazal (BEG) sub-basin consists of a number of rivers that originate from the Congo-Nile River divide and is made up of a large area of very low slope such that nearly all the basin runoff and precipitation is evaporated or leaked into swamps (i.e., about 96% is lost), with only about 0.5 km^3 leaving

6

the basin annually (Conway and Hulme , 1993). From the estimated GRACE-TWS patterns in Fig. (4, IC1), increased water storage for this region in the period between 2002 to 2003 at a rate of 64.4 mm/year was noticed. This could be explained by the increase in total annual rainfall between 2002-2004. Between 2003 and 2006, GRACE-TWS changes showed a reduction at a rate of 29.2 mm/year, again, inline with the noticeable reduction in total annual rainfall from TRMM. From 2006 to 2007, the stored water increased at a rate of 74.9 mm/year although the TRMM rainfall over this period does not show significant increase. This could imply reduced evaporation since the correlation between GRACE-TWS changes and the TRMM-rainfall over BEG gives a phase lag of 1-month at a maximum correlation of 0.53. For more details see the long paper.

4.2.2. The Ethiopian Highlands (EH); The Blue Nile

Analysing GRACE-TWS changes over Ethiopian Highlands (EH) (Fig. 4, IC2) showed a decline at a rate of 18.4 mm/year between 2002-2006. This decline can be explained by the temporal curve of the rainfall, which shows a decline in annual rainfall for the period 2002 to the end of 2005. A similar decline was noted by Di Baldassarre et al. (2011) who studied the changes in land cover, rainfall, and stream flow of Gilgel Abbay catchment, the largest contributor to the inflow of Lake Tana (the source of the upper Blue Nile; e.g., Conway and Hulme (1993)), and found that changes in streamflow records for the period 2001-2005 could have been attributed to changes in land cover, and changes in the annual and seasonal distribution of rainfall. Between 2006-2007, GRACE-TWS changes showed an increase in stored water at a rate of 44.3 mm/year. This could be attributed to the more than normal rainfall during the peak season of July-August as indicated by the amplitude of TRMM rainfall for 2006-2007.

ENSO is reported to have a reverse effect, i.e., deficient rainfall tends to occur during ENSO summers (e.g., Eltahir , 1996; Korecha and Barnston , 2007). Thus the Blue Nile sub-basin experienced drought episodes during ENSO warmer phases and enhanced rains during the ENSO cooler phases. Since 2006-2007 was an ENSO year in East Africa, one would expect less rainfall within the Blue Nile. The increase in the rainfall seen in TRMM's temporal graph (Fig. A2, IC2, in the paper), therefore, could be attributed to other factors such as the influence of IOD, given that this study obtained a correlation of 0.61 between the TRMM rainfall and IOD as opposed to 0.43 between TRMM and ENSO (results not shown).

For the Blue Nile sub-basin, Amarasekera et al. (1997) found a significant negative correlation between discharge and ENSO. For TWS, likewise, the positive correlations between ENSO and GRACE, i.e., (0.54 in Table 2), support the fact that ENSO is the dominant climate variability. However, the influence of IOD on TWS is also noticeable, i.e., 0.31 with respect to GRACE. With the removal of Lake Tana's signal, there is a shift in the GRACE signals (Fig. 5A) further towards the highlands.

7

The magnitude of the rate of change in stored water remains relatively the same (i.e., 44.3 mm/year) for the period April 2006 to December 2007 even after removing the signals of Lake Tana. For the period August 2002 to April 2006 and December 2007 to March 2012, the rate of decline in stored water within the highland is of the same order of magnitude as before the removal of Lake Tana's signal (e.g., 18.4 mm/year and 12.8 mm/year respectively). This further confirms the well known fact that the contribution of the Blue Nile's waters comes mainly from these highlands. This fact is supported by the computed correlations to climate variability, which increases slightly for IOD (0.47) but remains the same for ENSO (0.59, e.g., Table 2). The slight increase in correlation with IOD following the removal of Lake Tana's signals signifies that the stored water within the lake Tana dominates the entire sub-basin.

4.2.3. Lake Victoria Basin (LVB); The White Nile

Fig. 4 (spatial and temporal patterns of the third mode, IC3) presents the results of changes in water storage over LVB. From the spatial maps, GRACE-TWS changes indicate dominant anomalies over the western part of the Lake (Fig. 4, IC3). Looking at the spatial pattern of IC3 (Fig. 4) together with its associated temporal pattern, the most significant drop in water level within the basin occurred between October 2003 to the March 2006, consistent with the findings of Awange et al. (2008), Swenson and Wahr (2009) and Becker et al. (2010). The rate of fall in water computed for LVB within this period, for the data within our selected study area, was 84.5 mm/year. From March 2006 to May 2007, however, the TWS within LVB increased at a rate of 145.2 mm/year due to the ENSO related rainfall (i.e., Fig. A2, IC1 in the long-paper indicates an increase in the amplitude of rainfall between 2006-2007). Becker et al. (2010) who used the Global Precipitation Climatology Project (GPCP) observed an increase in precipitation from the end of 2005 to the beginning of 2007. For the study period, the correlations between GRACE-TWS changes and IOD was 0.48 and 0.56 with ENSO suggesting that both IOD and ENSO influence TWS changes in LVB.

In Fig. 5B, the contribution of Lake Victoria's signal is removed as discussed in section 3.2 in order to study the residual catchment's stored water signals. With the removal of the signals, the remaining catchment's signal in Fig. 5B indicate a similar behaviour for the period 2003-2004 and 2006-2007 before the signal was removed. The dominant GRACE signals appears on the western side of the catchment in line with TRMM rainfall data (IC1 in Fig. A2 in the long-paper), indicating the rainfall to be more towards the western side of the catchment. During the long rainy season of March-April-May (MAM), the western side of Lake Victoria receives more rainfall than the eastern part thus recharging the stored water causing an increase (cf. Awange et al., 2013a). Regarding the influence of climate variability on the catchment's stored water between 2002-2011, there is a decrease in correlations between ENSO (0.46) and GRACE-TWS changes after the removal of the Lake's signals (see Table 2). This could be attributed to the influence of climate variability on the rainfall that falls on the western side of Lake Victoria, which provides most of the source

of the stored water. In interpreting the results of the removed Lake's signals, however, it should be pointed out that remnant residual Lake's signals (e.g., Fig. 5B) also contribute to the correlation, hence any conclusion needs to be taken with care.

In contrast to the White Nile's water discharge from LVB, where the influence of ENSO climate variability has been shown to be weak (i.e., a weak negative association with ENSO; Eltahir (1996) and Amarasekera et al. (1997)), the influence of climate variability on TWS changes within the basin is strong (see Table 2). LVB's general TWS trend showed a decline even after the 2007 ENSO that saw a rise in its TWS. This general decline impacts upon the entire Nile Basin as evident from the water levels of Lake Nasser (e.g., as reported also in Becker et al. (2010) and Crétaux et al. (2011)), which follows the pattern of Lake Victoria even though the Blue Nile contributes most of the Nile's waters serving Egypt and Sudan.

4.2.4. Lake Nasser region

For this region, the ICA-derived GRACE-TWS anomalies were localized to the northwest-southeast direction of the Red Sea (Fig. 4, IC4). This signal could be largely attributed to the water storage changes within the Red Sea and Lake Nasser and thus needs to be removed. The use of altimetry data to remove the dominant GRACE signals from the Red Sea is supported by a correlation of 0.71 between GRACE-TWS changes and the altimetry data for the Red Sea. Altimetry observations provided by NOAA ERDDAP (the Environmental Research Division's Data Access Program program)[6] over the Red Sea were converted to EWT changes (see the conversion procedure in section 3.1.1) and scaled by its variance to unit-variance (i.e., IC4 of GRACE, c.f., Fig. 4D). Some differences in amplitude were detected (compare the amplitudes of red and blue in Fig. 6C) mainly in 2004, 2005, and after 2008. The residual of GRACE-TWS changes minus Red Sea-EWT is shown in black. Lake Nasser's altimetry are also converted into EWT time series (same procedure as for the Red Sea), the results of which are shown in cyan. As can be seen, after 2008, the EWT changes corresponding to Lake Nasser is very similar to the residuals (the black line; Fig. 6C).

After the removal of the dominant signal of the Red Sea, the resulting signal (c.f. Fig. 6A) indicates a decline in stored water in the Western Plateau within the Nubian Aquifer covering Lake Nasser at a rate of 2.6 mm/year. The loss of water in this region is attributed by Sultan et al. (2012) to the fact that most of the water is extracted from the Nubian Aquifer and used for agricultural purposes. No dominant independent pattern was observed from TRMM and GLDAS data over the region surrounding lake Nasser, indicating that precipitation and soil moisture changes during the study period 2002-2011 was not the source of the observed TWS changes (see Fig. 6A). This supports the fact that the stored water within the Lake Nasser basin originates from the other Nile

---

[6]$http://coastwatch.pfeg.noaa.gov$

sub-basins. A weak negative correlations was observed between GRACE-TWS and ENSO (-0.10) for the study period. During the same period, the correlation between GRACE and IOD was 0.13. Without the Red sea and Lake Tana's signals, correlations between IOD and ENSO on the one hand and GRACE-TWS changes on the other hand were respectively 0.33 and 0.30, thus following closely to the LVB pattern (i.e., 0.48 and 0.46 for IOD and ENSO, respectively, for the same).

FIGURE 6

TABLE 2

5. Conclusion

Using the ICA method (Spatial ICA in Forootan and Kusche , 2012; Forootan et al. , 2012), we were able to extract independent water storage patterns of the Nile sub-basins and relate them to climate variability over the study period 2002-2011. For the individual sub-basins, the study found that:

1. The stored water within LVB could have been influenced both by anthropogenic as well as climate variability (ENSO and IOD). The removal of the dominant Lake Victoria signal shows the western side of Lake Victoria having increased TWS, a possible consequence of the long rains of the MAM season that pounds the western side of the lake more.

2. Ethiopian Highlands (EH) experienced a general reduction in rainfall as seen from the TRMM data over the study period from 2002 to the end of 2010, with the period between 2005-2010 recording low rainfall during the long rainy season of JJAS and low total annual rainfall, a possible explanation for the 2011 drought that hit the Greater Horn of Africa (GHA). This reduction in rainfall impacts on TWS changes over the GHA as seen from GRACE outputs (see also Omondi et al. , 2013a).

3. Bar-el-Ghazal region showed a mixed increase/decrease in the stored water associated with increase/decrease in rainfall at different times of the study period. The dominant climate variability in the region was found to be ENSO.

4. For the Lake Nasser region, it is clear that the dominant EWT changes of the Red Sea obscure the real impact of over extraction of water in the Nubian aquifer region for irrigation purposes (e.g., Sultan et al. , 2012). The situation is not helped much by the fact that there could be insufficient recharge from the south-north flow of the groundwater due to the presence of the Uweinat-Aswan uplift.

5. In general, for almost all the sub-basins, the dominant climate variability on GRACE-TWS changes was the ENSO, with the exception of LVB and EH where the influence of IOD on GRACE-TWS changes was noticeable.

10

Acknowledgments

References

Amarasekera, K.N., Lee, R.F., Williams, E.R., Eltahir, E.A.B. (1997). ENSO and the natural variability in the flow of tropical rivers. Journal of Hydrology, 200, 24-39, doi:10.1016/S0022-1694(96)03340-9.

Awange, J.L., Anyah R, Agola N, Forootan E, Omondi, P. (2013a). Potential impacts of climate and environmental change on the stored water of Lake Victoria Basin and economic implications. Water Resources Research, 49, 8160-8173, doi: 10.1002/2013WR014350.

Awange, J.L., Forootan, E., Fleming, K., Omondi, P., and Odhiambo, G., (2013b). Dominant patterns of water storage changes in the Nile basin, during 2003-2013. AGU books: Chapman Conference on Remote Sensing of Terrestrial Waters in Hawaii, USA, in press.

Awange, J.L., Fleming, K.M., Kuhn, M., Featherstone, W.E., Heck, B., Anjasmara, I. (2011). On the suitability of the $4^{o} \times 4^{o}$ GRACE mascon solutions for remote sensing Australian hydrology. Remote Sensing of Environment, 115, 864-875, doi: 10.1016/j.rse.2010.11.014.

Awange, J.L., Sharifi, M.A., Baur, O., Keller, W., Featherstone, W., Kuhn, M. (2009). GRACE hydrological monitoring of Australia: current limitations and future prospects. Journal of Spatial Science, 54 (1), 23-36, doi:10.1080/14498596.2009.9635164.

Awange, J.L., Sharifi, M.A., Ogonda, G., Wickert, J., Grafarend, E., Omulo, M. (2008). The Falling Lake Victoria Water Levels: GRACE, TRIMM and CHAMP satellite analysis of the lake Basin. Water Resource Management 22, 775-796, doi:10.1007/s11269-007-9191-y.

Awange, J.L., Ong'ang'a, O. (2006). Lake Victoria: Ecology Resource and Environment. Springer-Verlag, Berlin, 354pp.

Anyah, R.O., Semazzi, F.H.M. (2006). NCAR-AGCM ensemble simulations of the variability of the Greater Horn of Africa climate, Special Issue, Theoretical and Applied Climatology, 86, 39-62.

Aus der Beek, T., Menzel, L., Rietbroek, R., Fenoglio-Marc, L., Grayek, S., Becker, M., Kusche, J., Stanev, E. (2012). Modeling the water resources of the Black and Mediterranean Sea river basins and their impact on regional mass changes. Journal of Geodynamics, 59-60, 157-167, doi:10.1016/j.jog.2011.11.011.

Becker, M., LLovel, W., Cazenave, A., Güntner, A., Crétaux, J-F. (2010). Recent hydrological behavior of the East African great lakes region inferred from GRACE, satellite altimetry and rainfall observations. C. R. Geoscience, 342, 223-233, http://dx.doi.org/10.1016/j.crte.2009.12.010.

Behera, S.K, Luo, J.J., Masson, S., Delecluse, P., Gualdi, S., Navarra, A. (2005). Paramount Impact of the Indian Ocean Dipole on the East African short Rains: ACGCM study. J. Climate, 18, 41-54.

Berhane, G., Kristine, M., Nawal.,A. and Kristine W., (2013). Water leakage investigation of micro-dam reser-voirs in Mesozoic sedimentary se- quences in Northern Ethiopia. Journal of African Earth Sciences,79:98- 110, http://dx.doi.org/10.1016/j.jafrearsci.2012.10.004

Beyene, T. Lettenmaier, D.P., Kabat, P. (2010). Hydrologic impacts of climate change on the Nile River Basin: implications of the 2007 IPCC scenarios. Climatic Change 100, 433-461, doi:10.1007/s10584-009-9693-0.

Black, E, Slingo, J., Sperber, K.R. (2003) An observational study of the relationship between excessively strong short rains in the coastal East Africa and Indian Ocean SST., Mon Wea. Rev. 131, 74-94.

Block, P.J., Strzepek, K., Rajagopalan B. (2007). Integrated management of the Blue Nile basin in Ethiopia. Hy-dropower and Irrigation Modeling. International Food Policy Research Institute, IFPRI Discussion Paper 00700.

Bonsor, H.C., Mansour, M.M., MacDonald, A.M., Hughes, A.G., Hipkin, R.G., Bedada, T. (2010). Interpretation of GRACE data of the Nile Basin using a groundwater recharge model. Hydrology and Earth System Sciences Discussions 7, 4501-4533, doi:10.5194/hessd-7-4501-2010.

Clark, C.O., Webster, P.J., Cole, J.E. (2003). Interdecadal variability of the relationship between the Indian Ocean zonal mode and East African coastal rainfall anomalies. J. Clim. 16, 548-554.

Colberg, F., Reason, C.J.C. (2004). South Atlantic response to El-Nino-Southern Oscillation induced climate variability in an ocean general circulation model. J. Geophys. Res., 109, C12015, 14pp

Conway, D. (2005). From headwater tributaries to international river: Observing and adapting to climate variability and change in the Nile Basin. Global Environmental Change 15, 99-114, doi:10.1016/j.gloenvcha.2005.01.003.

Conway, D., Hulme, M. (1993). Recent fluctuations in precipitation and runoff over the Nile sub-basins and their impact on main Nile discharge. Climatic Change 25:127-151, doi: 10.1007/BF01661202.

Crétaux J.F., Jelinski, W., Calmant, S., Kouraec, A., Vuglinski, V., Bergé-Nguyen, M., Gennero, M.-C., Nino, F., Abarca Del Rio, R., Cazenave, A., Maisongrande, P. (2011). SOLS: A lake database to monitor in the Near real-time water level and storage variations from remote sensing data. Advances in Space Research, 47 1497-1507, doi:10.1016/j.asr.2011.01.004.

Destouni, G., Jaramillo, F., Prieto, C. (2013). Hydroclimatic shifts driven by human water use for food and energy production. Nature Climate Change 3, 213-217, doi:10.1038/nclimate1719

Di Baldassarre, G., Elshamy, M., van Griensven, A., Soliman, E., Kigobe, M., Ndomba, P., Mutemi, J., Mutua, F., Moges, S., Xuan, J.-Q., Solomatine, D., Uhlenbrook, S. (2011). Future hydrology and climate in the River Nile basin: a review. Hydrol. Sci. J. 56(2), 199-211, doi:10.1080/02626667.2011.557378.

Eltahir, E.A.B. (1996). El Niño and the natural variability in the flow of the Nile River. Water Resour. Res. 32 (1), 131-137.

Flechtner, F. (2007). GFZ Level-2 processing standards document for level-2 product release 0004, GRACE 327-743, Rev. 1.0.

Fleming K.M, Awange J.L., Kuhn, M., Featherstone, W.E. (2012). Evaluating the TRMM 3B43 monthly precipitation product using gridded rain-gauge data over Australia. Australian meteorological and oceanographic Journal, 63, 421-426.

Forootan, E., Awange, J.L., Kusche, J., Heck, B., Eicker, A. (2012). Independent patterns of water mass anomalies over Australia from satellite data and models. Remote Sensing of Environment, 124, 427-443, doi:0.1016/j.rse.2012.05.023.

Forootan E., Rietbroek, R., Kusche, J., Sharifi, M.A., Awange, J.L., Schmidt, M., Omondi, P., Famiglietti, J. (2014). Separation of large scale water storage patterns over Iran using GRACE, altimetry and hydrological data. Remote Sensing of Environment, 140, 580-595, dx.doi.org/10.1016/j.rse.2013.09.025.

Forootan, E., Kusche, J. (2013). Separation of deterministic signals, using independent component analysis (ICA). Stud. Geophys. Geod, 57, 17-26, doi: 10.1007/s11200-012-0718-1.

Forootan, E., Kusche, J. (2012). Separation of global time-variable gravity signals into maximally independent components. Journal of Geodesy, 86 (7), 477-497, doi:10.1007/s00190-011-0532-5.

García-García, D., Ummenhofer, C.C., Zlotnicki, V. (2011). Australian water mass variations from GRACE data linked to Indo-Pacific climate variability. Remote Sensing of Environment, 115, 2175-2183, doi:10.1016/j.rse.2011.04.007.

Ghoubachi, S.Y. (2010). Impact of Lake Nasser on the groundwater of the Nubia sandstone aquifer system in Tushka area, south western desert, Egypt, Journal of King Saud University - Science, doi: 10.1016/j.jksus.2010.04.005.

Indeje, M., Semazzi, F.H.M., Ogallo, L.J. (2000). ENSO signals in East African rainfall seasons. Int. J. Climatology, 20, 19-46.

Konar, M., Todd, M.J., Muneepeerakul, R., Rinaldo, A., Rodriguez-Iturbe, I. (2013). Hydrology as a driver of biodiversity: Controls on carrying capacity, niche formation, and dispersal. Advances in Water Resources, 51, 317-325, http://dx.doi.org/10.1016/j.advwatres.2012.02.009.

Korecha, D., Barnston, A. (2007). Predictability of June-September Rainfall in Ethiopia. Monthly Weather Review 135: 628-650, doi:10.1175/MWR3304.1.

Kumar, S.V., Peters-Lidard, C.D., Tian, Y., Houser, P.R., Geiger, J., Olden, S., Lighty, L., Eastman, J.L., Doty, B., Dirmeyer, P., Adams, J., Mitchell, K., Wood, E.F., Sheffield, J. (2006). Land information system: An interoperable framework for high resolution land surface modeling, Environmental Modelling & amp; Software 21 (10), 1402-1415, doi:10.1016/j.envsoft.2005.07.004.

Kummerow, C., Barnes, W., Kozu, T., Shiue, J. Simpson, J. (1998). The Tropical Rainfall Measuring Mission (TRMM) sensor package. Journal of Atmospheric and Oceanic Technology 15 (3), 809-817, doi:10.1175/1520-0426(1998)015<0809:TTRMMT>2.0.CO;2.

Kusche, J. (2007). Approximate decorrelation and non-isotropic smoothing of time-variable GRACE-type gravity field models. Journal of Geodesy, 81, 733-749, doi:10.1007/s00190-007-0143-3.

Kusche, J., Schmidt, R., Petrovic, S., Rietbroek, R. (2009). Decorrelated GRACE time-variable gravity solutions by GFZ, and their validation using a hydrological model. Journal of Geodesy, 83, 903-913, doi:10.1007/s00190-009-0308-3.

Lehmann, E.L., D'Abrera, H.J.M. (1998). Nonparametrics: statistical methods based on ranks. rev. ed. Englewood Cliffs, NJ: Prentice-Hall, 464 pages. ISBN 978-0-387-35212-1.

Longuevergne, L., Wilson, C.R., Scanlon, B.R., Crétaux J.F. (2012). GRACE water storage estimates for the Middle East and other regions with significant reservoir and lake storage. Hydrol. Earth Syst. Sci. Discuss., 9, 11131-11159, doi:10.5194/hessd-9-11131-2012.

Mohamed, Y.A., Savenije, H.H.G., Bastiaanssen, W.G.M., van den Hurk, B.J.J.M. (2006). New lessons on the Sudd hydrology learned from remote sensing and climate modeling. Hydrology and Earth System Sciences, Vol. 10: 507-518.

Naumann, G., Barbosa, P., Carro, H., Singleton, A., Vogt, J. (2012). Monitoring drought conditions and their uncertainties in Africa using TRMM Data. J. Appl. Meteor. Climatol., 51, 1867-1874. doi:http://dx.doi.org/10.1175/JAMC-D-12-0113.1.

Nicholson, S., Some, B., McCollum, J., Nelkin, E., Klotter, D., Berte, Y., Diallo, B., Gaye, I., Kpabeba, G., Ndiaye, O., Noukpozounkou, J., Tanu, A., Thiam, A., Toure, A.A., Traore, A. (2003). Validation of TRMM and other rainfall estimates with a high-density gauge dataset for West Africa: Part II: Validation of TRMM rainfall products. Journal of Applied Meteorology 42(10), 1355–1368, doi:10.1175/1520–0450(2003)042<1355:VOT.

Omondi, P., Awange, J., Forootan, E., et al. (2013a). Changes in temperature and precipitation extremes over the Greater Horn of Africa region from 1961 to 2010. International Journal of Climatology, doi: 10.1002/joc.3763.

Omondi, P., Awange, J., Ogallo, Ininda, J., Forootan, E. (2013b). The influence of low frequency sea surface temperature modes on delineated decadal rainfall zones in Eastern Africa region. Advances in Water Resources, dx.doi.org/10.1016/j.advwatres.2013.01.001.

Omondi, P., Awange, J., Ogallo, L.A., Okoola, R.A., Forootan, E. (2012). Decadal rainfall variability modes in observed rainfall records over East Africa and their relations to historical sea surface temperature changes. Journal of Hydrology, Vol.464-465, Page 140-156, dx.doi.org/10.1016/j.jhydrol.2012.07.003.

Rientjes, T.H.M.,Haile, A.T., Kebede, E., Mannaerts, C. M. M., Habib, E., Steenhuis, T. S. (2011). Changes in land cover, rainfall and stream flow in Upper Gilgel Abbay catchment, Blue Nile basin - Ethiopia. Hydrol. Earth Syst. Sci., 15, 1979-1989, doi:10.5194/hess-15-1979-2011.

Rieser, D., Kuhn, M., Pail, R., Anjasmara, I., Awange, J.L. (2010). Relation between GRACE-derived surface mass variations and precipitation over Australia. Australian Journal of Earth Science 57 (7), 887-900, doi:10.1080/08120099.2010.512645.

Rodell, M., Famiglietti, J.S. (2001). An analysis of terrestrial water storage variations in Illinois with implications for the gravity recovery and climate experiment (GRACE). Water Resourc. Res. 37, 1327-1340, doi:10.1029/2000WR900306.

Rodell M, Houser, P.R., Jambor, U., Gottschalck, J., Mitchell, K., Meng, K., Arsenault, C.-J., Cosgrove, B., Radakovich, J., Bosilovich, M., Entin, J.K., Walker, J.P., Lohmann, D., Toll, D. (2004). The Global Land Data Assimilation System. Bulletin of the American Meteorological Society, 85 (3), 381-394.

Sahin, M. (1985). Hydrology of the Nile Basin. Developments in water Science No. 21. Elsevier, New York 575 pp.

Saji, N.H., Goswami, B.N., Vinayachandran, P.N., Yamagata, T. (1999). A dipolemode in the tropical Indian Ocean. Nature, 401, 360-363. http://dx.doi.org/10.1038/43854.

Saji, N.H., Yamagata, T. (2003a) Possible impacts of Indian Ocean Dipole Mode events on global climate. Climate Research, 25 (2), 151-169.

Saji, N.H., Yamagata, T. (2003b) Structure of SST and Surface Wind Variability during Indian Ocean Dipole Mode Events: COADS Observations. J. Climate, 16 (16), 2735-2751.

Salem, O. M., and P. Pallas (2002), The Nubian Sandstone Aquifer System, paper presented at Managing Shared Aquifer Resources in Africa, ISARM-AFRICA, Tripoli, Libya, 2-4 June 2002.

Salem, O. M. (2007), Management of Shared Groundwater Basins in Libya, African Water Journal, 1(1), 109-120.

Sefelnasr A.M. (2007). Development of groundwater flow model for water resources management in the development areas of the western desert, Egypt. Dissertation, Faculty of Natural Sciences III of the Martin Luther University Halle-Wittenberg.

Senay, G.B., Asante, K., Artan, G. (2009). Water balance dynamics in the Nile Basin. Hydrological Processes 23, 3675-3681, doi:10.1002/hyp.7364.

Song, Q., Vecchi, G.A., Rosati, A.J. (2007). Indian Ocean Variability in the GFDL Coupled Climate Model. J. Climate, 20, 2895-2916

Sultan, M., Ahmed, M., Sturchio, N., Yan, Y.E., Milewski, A., Becker, R., Wahr, J., Becker, D., Chouinard, K. (2012). Assessment of the vulnerabilities of the Nubian sandstone fossil aquifer, North Africa. Water Encyclopedia, in press, Elsevier.

Sutcliffe, J.V., Parks, Y.P. (1999). The hydrology of the Nile, IAHS Special publication No. 5. IAHS press, Institute of Hydrology: Wallingford, Oxford Shine.

Swenson, S., Wahr, J., Milly, P. (2003). Estimated accuracies of regional water storage variations inferred from the Gravity Recovery and Climate Experiment (GRACE). Water Resources Research, 39(8), 1223, doi:10.1029/2002WR001808.

Swenson, S., Wahr, J. (2002). Methods for inferring regional surface-mass anomalies from Gravity Recovery and Climate Experiment (GRACE) measurements of time-variable gravity. Journal of Geophysical Research: Solid Earth, 107(B9):2193.

Swenson, S., Wahr, J. (2009). Monitoring the water balance of Lake Victoria, East Africa, from space. Journal of Hydrology 370(1-4), 163-176, doi:10.1016/j.jhydrol.2009.03.008.

Tapley, B.D., Bettadpur, S., Ries, J.C., Thompson, P.F., Watkins, M. (2004). GRACE measurements of mass variability in the Earth system. Science 305, 503-505, doi:10.1126/science.1099192.

Wahr, J., Molenaar, M., Bryan, F. (1998). Time variability of the Earth's gravity field: Hydrological and oceanic effects and their possible detection using GRACE. Journal of Geophysical Research 103 (B12), 30205-30229, DOI:10.1029/98JB02844.

Yates, D.N., Strzepek, K.M. (1998). Modelling the Nile Basin under climate change. Journal of Hydrologic Engineering 3(2), 98-108, doi:10.1061/(ASCE)1084-0699(1998)3:2(98).

Table 1: Characteristics of the Nile sub-basins

	Area	Catchment	Remark
Lake Victoria	258,000 km^2	Lakes Kyoga (75,000 km^2) Albert, Elbert, George (48,000 km^2)[a] Semiliki Basin	Head Waters of the While Nile
Barrel-Ghazel (BEG)	526,000 km^2	Congo-Nile River divide Large area of low slope	About 96%[b] of basin runoff and precipitation is lost to evaporation and leakage to swamp
Ethiopian Highland (EH)	300,000 km^2	Lake Tana Region (20000 km^2) Upper Blue Nile region (150,000 km^2) Lower Blue Nile region (60,000 km^2) Dinda Rahad region (60,000 km^2)	Head waters[a] of the Blue Nile contributing about 65% of the Nile waters.
Egypt Desert Region		Lake Nasser (formed by Aswan dam)	Water loss due to evaporation

[a] Yates (1998)
[b] Conway and Hulme (1993)

Table 2: Correlation coefficient between independent patterns of TWS derived from GRACE and climate variability of IOD (in bold) and ENSO (in normal text) over the Nile sub-basins. Correlations are computed at 95% level of confidence. The insignificant values are morked.

Basin	Correlation
Barh-El-Ghazal IC1 GRACE	+**0.18** (insignificant) +0.71
Ethiopian Highlands (with the red Sea and the lake's signals) IC2 GRACE	+**0.31** +0.54
Ethiopian Highlands (without the red Sea and the lake's signals) IC2 GRACE	+**0.47** +0.59
Lake Victoria Basin (with the red Sea and the lake's signals) IC3 GRACE	+**0.48** 0.56
Lake Victoria Basin (without the red Sea and the lake's signals) IC3 GRACE	+**0.48** 0.46
The Nasser region (with the red Sea and the lake's signals) IC4 GRACE	+**0.13** (insignificant) −0.10 (insignificant)
The Nasser region (without the red Sea and the lake's signals) IC4 GRACE	+**0.33** +0.30

Advances in Water Resources
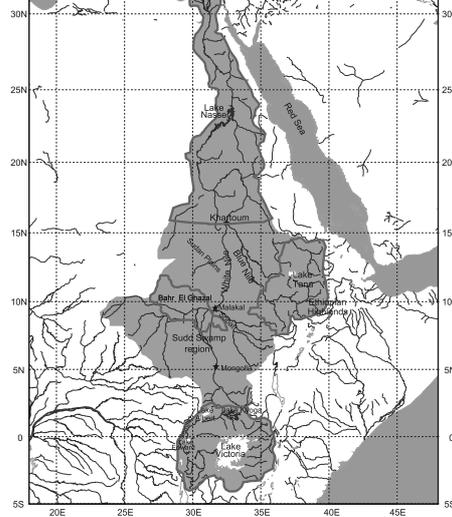
Figure 1: The Nile Basin (brown shaded region) with the major sub-basins used in the study shown.
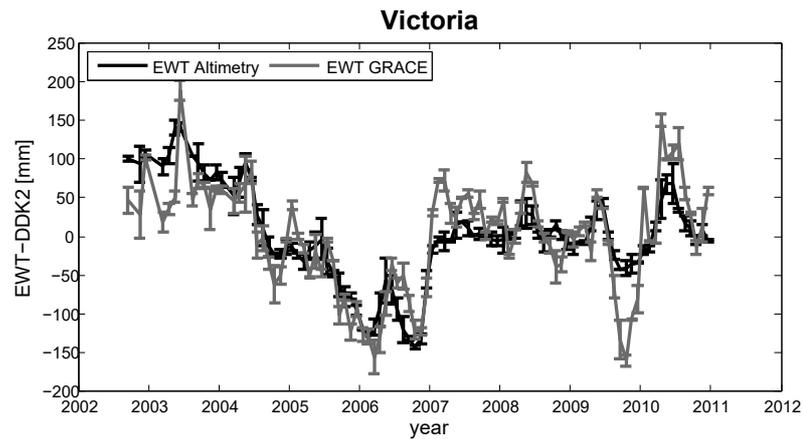
Figure 2: Satellite altimetry-derived signals for Lake Victoria (after smoothing with the DDK2 filter (Kusche et al. , 2009) and conversion to equivalent water thickness (EWT)). Both time series are centered with respect to their temporal means. The altimetry derived EWT signals represents a smoother pattern compared to the GRACE signals, which might be due to the fact that it contains only water level changes of Lake Victoria and not water storage changes over the surrounding regions of the lake. Error-bars for the GRACE-derived TWS are obtained by propagating the errors of spherical harmonics, after DDK2 filtering, to TWS without considering the covariances. Computing the error-bars for altimetry-derived TWS is done by considering the accuracy provided in LEGOS data (Crétaux et al. , 2011)

Advances in Water Resources

RMS of the introduced anomalies
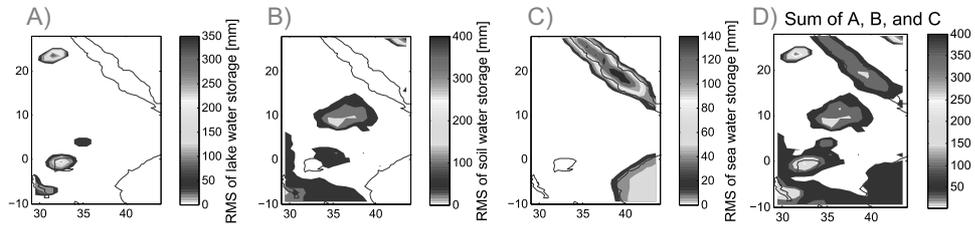
Results of ICA
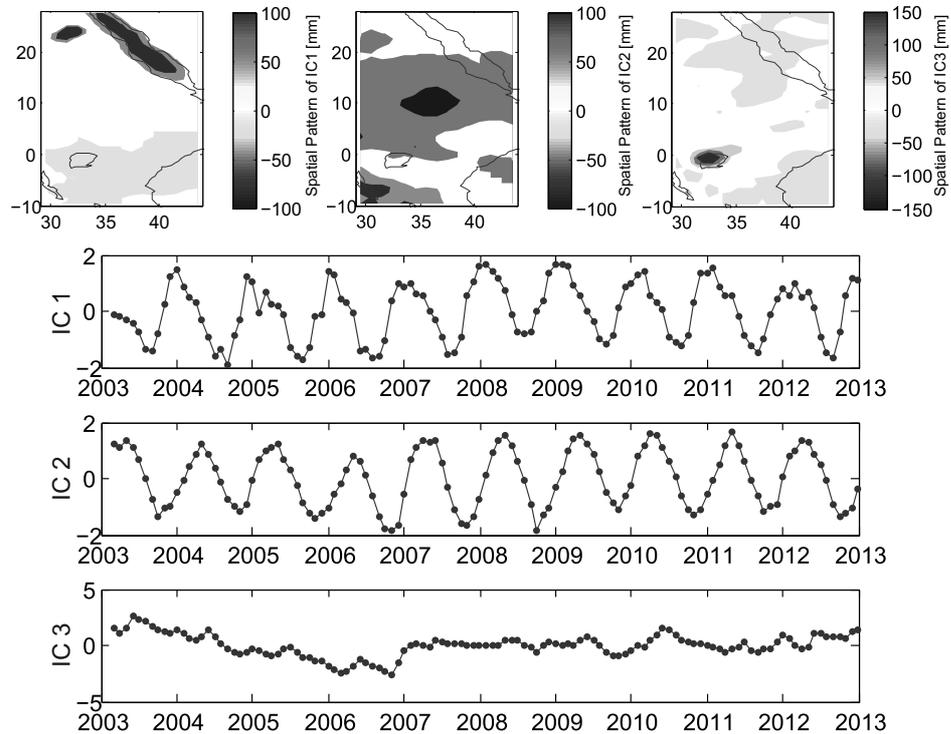
Figure 3: (top) Root mean squares of the introduced water storage changes over the major lakes of the Nile Basin, soil moisture changes of the basin and non-tidal water storage changes of the Red Sea; (Bottom) The first three independent modes, derived from ICA. The results show that the strong signal of Lake Victoria (IC3) can successfully be separated from those of the Red Sea and Lake Nasser (IC1) and those of soil moisture (IC2).

16
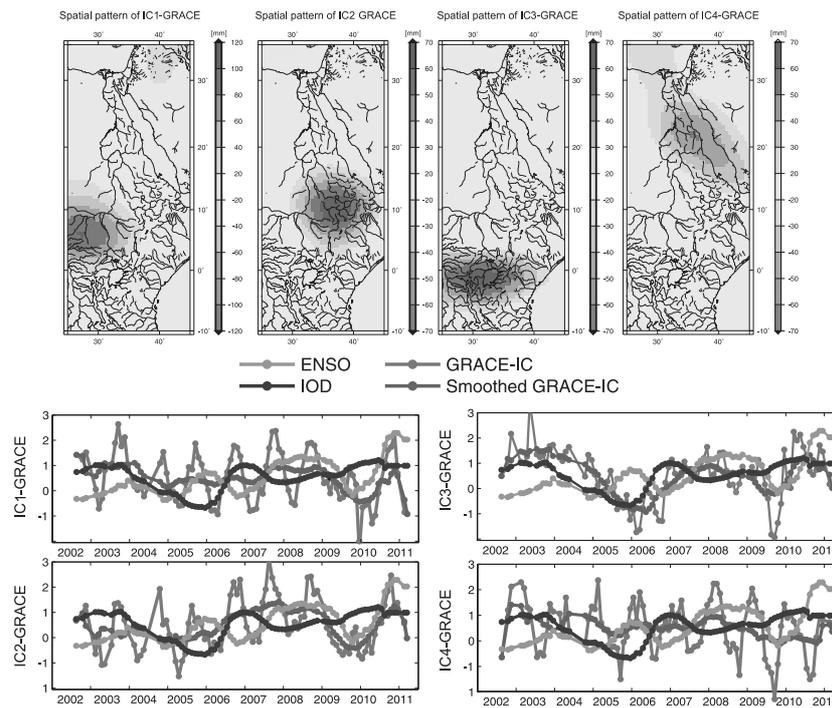
Figure 4: ICA decomposition of GRACE TWS signal within the Nile Basin using the proposed ICA method of Forootan and Kusche (2012, 2013). The upper panels are the spatial pattern of each IC. Note that the Nile Basin's TWS signal is separated (localized) by the ICA method into 4 significant spatially independent components (BEG (left), EH (second from left), LVB (third from left) and Red Sea (right). Together, these four signals computed over the Nile Basin account for 92% of cumulative total variance of TWS changes. In the lower panel, their corresponding time series (ICs) overlaid on smoothed time series of the loading, as well as ENSO and IOD indices.
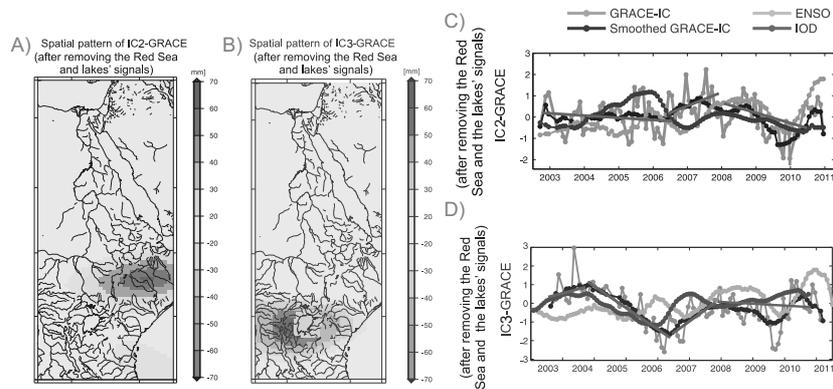
Figure 5: Dominant independent patterns of GRACE TWS after removing the contribution of Lakes Tana and Victoria surface water signals. Spatial patterns show the concentration of the remaining signals (after removal) over the Ethiopian Highlands (panel A) and the western part of Lake Victoria Basin (panel B). Panels C and D shows their corresponding time series (ICs) overlaid on smoothed time series of the loading and ENSO and IOD

Advances in Water Resources
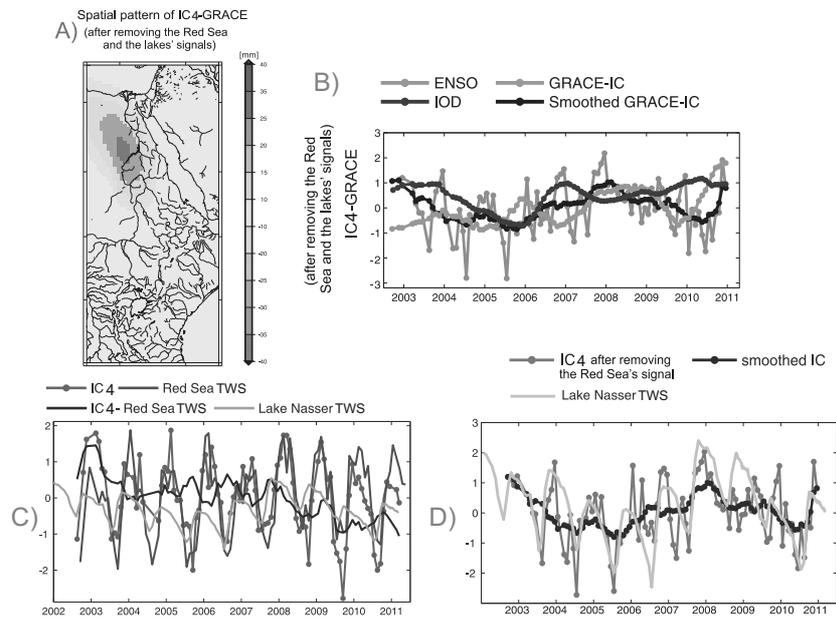
Figure 6: Dominant independent pattern of GRACE-TWS changes for the Nasser region. A) Spatial pattern of IC4 derived from GRACE-TWS changes after correction for the water storage changes of the Red Sea; B) the corresponding temporal evolution of (A) and its comparison with the ENSO and IOD indices; C) comparison of IC4 in (B) with the signal of the Red Sea and Lake Nasser; and D) an overview of IC4 after removing the signal of the Red Sea and its comparison with the signal of Lake Nasser. We should mention here that the Lake Nasser TWS of (C) and (D) represent the same quantity. To enhance the visual comparison, that of (D), is however, vertically shifted to the mean of IC4